Accurate predictions of chaotic motion of a free fall disk

Tianzhuang Xu (徐天壮), Jing Li (李靖), Zhihui Li (李志辉), and Shijun Liao (廖世俊)

COLLECTIONS

This paper was selected as Featured

View Online

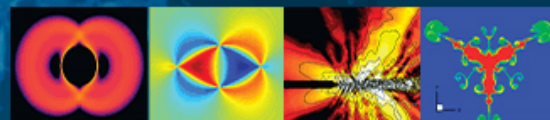Export Citation

CrossMark

Accurate predictions of chaotic motion of a free fall disk Ⓕ

Tianzhuang Xu (徐天壮),[1] Jing Li (李靖),[1,a] Zhihui Li (李志辉),[2,3] ⓘD and Shijun Liao (廖世俊)[1,4,a] ⓘD

AFFILIATIONS

[1] Center of Advanced Computing, School of Naval Architecture, Ocean and Civil Engineering, Shanghai Jiaotong University, 200240 Shanghai, China
[2] National Laboratory for Computational Fluid Dynamics, 100191 Beijing, China
[3] China Aerodynamics Research and Development Center, 621000 Mianyang, China
[4] School of Physics and Astronomy, Shanghai Jiaotong University, 200240 Shanghai, China

[a] Authors to whom correspondence should be addressed: lijing_@sjtu.edu.cn and sjliao@sjtu.edu.cn

ABSTRACT

It is important to know the accurate trajectory of a free fall object in fluid (such as a spacecraft), whose motion might be chaotic in many cases. However, it is impossible to accurately predict its chaotic trajectory in a long enough duration by traditional numerical algorithms in double precision. In this paper, we give the accurate predictions of the same problem by a new strategy, namely, the Clean Numerical Simulation (CNS). Without loss of generality, a free-fall disk in water is considered, whose motion is governed by the Andersen–Pesavento–Wang model. We illustrate that convergent and reliable trajectories of a chaotic free-fall disk in a long enough interval of time can be obtained by means of the CNS, but different traditional algorithms in double precision give disparate trajectories. Besides, unlike the traditional algorithms in double precision, the CNS can predict the accurate posture of the free-fall disk near the vicinity of the bifurcation point of some physical parameters in a long duration. Therefore, the CNS can provide reliable prediction of chaotic systems in a long enough interval of time.

Published under license by AIP Publishing. https://doi.org/10.1063/5.0039688

I. INTRODUCTION

Free-fall motion widely exists in nature and industry. For example, falling leaves and feathers are the common phenomena for people to see in daily life. A very important application is the spacecraft re-entry since some objects are massive in size and high-temperature resistant, and the re-entry may cause structural, environmental, and safety issues on the Earth's surface. Recently, the re-entry of China's Tiangong-1 spacecraft has drawn much attention to accurately predicting the uncontrolled trajectories.[1] The six degrees of freedom (DoF) orbit model is the standard model describing this problem.[2,3] Nevertheless, accurately modeling a free-falling process is quite challenging by the 6 DoF model. The chaotic features inherent of this system strongly depend on initial conditions (SDIC)[4] and, hence, are a great threat to numerical calculations.

Unfortunately, traditional numerical methods are naturally not "clean." More or less noises (i.e., truncation errors and round-off errors) are found during the calculation. These noises will increase exponentially in chaotic cases, due to the SDIC, which was first discovered by Poincaré[5] in 1890 and developed by Lorenz[6] in 1963, i. e., the so-called "butterfly effect." Thus, for a chaotic dynamic system, a tiny variation of the initial condition can result in significant differences between numerical trajectories after a long-time simulation.[7,8] Furthermore, Lorenz[9] reported that it is also sensitive to the numerical algorithm. He found that the (maximum) Lyapunov exponent alters between negative and positive values even when the time step is very small. Teixeira *et al.*[10] further investigated the time step sensitivity of three non-linear atmospheric models utilizing traditional algorithms in double precision. They made a somewhat pessimistic conclusion that "for chaotic systems, numerical convergence cannot be guaranteed forever."

In fact, the free-fall problem itself has been experiencing a long and complicated history until a widely accepted theory emerges. The qualitative discussion of it can date back to Maxwell.[11] At that time, little was known about the nature of the transitions between different modes. Many simple shapes, such as disks, cylinders, polygons, cones, and even particles, have been studied via experiments or numerical

simulations of Navier–Stokes equations, and complex falling modes were discovered, including tumbling, fluttering, steady, and chaotic postures.[12–18] Among these shapes, the disk is the most well-studied subtopic in this field. A few analytical models developed by researchers greatly enhanced the understanding of free-fall motion in fluids and promised the possibility to predict the falling without solving the Navier–Stokes equations, which are notorious for the high computational cost. Kuznetsov[19] organized a comprehensive summary on that topic.

A direct way to reveal the rules is the experiment. As for the free-fall motion of disks, it mainly focuses on the relationships between physical parameters and falling modes. Willmarth et al. designed a series of experiments and measured a phase diagram of fluttering, tumbling, and steady descent according to six related physical parameters.[20] By dimensional analysis, three similarities were obtained, and with small ratios between the thickness and the diameter of the disk, falling modes only depend on the dimensionless moment of inertia and the Reynolds number. Field et al. further found a chaotic transition region between fluttering and tumbling.[21] Zhong et al. recently conducted the most comprehensive experimental research on free-fall thin disks. They closely studied the relationships between fluttering (zigzag in their words) free-fall motion and the Reynolds number. They found a critical Reynolds number of $Re_{cr} \approx 2000$. The oscillatory amplitude is proportional to Re below Re_{cr} while invariant beyond Re_{cr}.[22] Zhong et al. also researched the mechanism of how two-dimensional fluttering modes transform to three-dimensional spiral modes.[23,24] Their experimental results have been numerically confirmed with an immersed boundary-lattice Boltzmann flux solver.[25,26] Based on the three-dimensional spiral modes, Kim et al. further studied the free-fall motion of a pair of rigidly linked disks. They discovered a mutative falling mode with two disks falling in helical and conical motions.[27] Recently, Lee et al. also studied the bristled disk where they found that the bristled structure of disks could strengthen the stability of free-fall motion.[28]

Naturally, analytical models were built to explain the various modes and the bifurcation. Kirchhoff made a pioneering distribution by deriving finite-dimensional governing equations,[29] called Kirchhoff equations, based on an important fact that velocities of the solid body moving in an ideal incompressible fluid can be decoupled from the field equations of the fluid itself. Nevertheless, Kirchhoff equations are only related to ideal fluid corresponding to conservative systems without considering dissipation. It can describe the steady fall regimes and how to sustain regular or chaotic oscillations and rotations,[30,31] but still far away from the real motion. Inherited from Kirchhoff equations, many researchers tried to introduce appropriate amendments to build a better model, especially on replicating the fluttering, tumbling, stable, and chaotic falling modes and also manifesting the bifurcation structure between fluttering and tumbling. There are two models with significant importance, and we introduce them briefly. The first is the Tanabe–Kaneko model.[32] This model first introduces the Joukowsky theorem to introduce the effect of circulation and implements a sign function to relate the lift term to the kinematic information of a disk. Tanabe and Kaneko explained that the introduction of Joukowsky theorem may give rise to complex dynamics and chaos during falling in a fluid due to gravity and expressed the circulation with a sign function. Although there was some incorrectness of the Tanabe–Kaneko formulation, including that they omitted the effect of added mass and

Archimedean buoyancy and there was some contradiction between the coefficients, which was criticized after publication,[33,34] the Tanabe–Kaneko model qualitatively gives a reasonable picture of possible regimes of complex dynamics for a disk falling in a fluid. Andersen, Pesavento, and Wang proposed a more elaborate model to describe the fall of a flat disk or a body with an elliptic profile in a fluid through a finite-dimensional model.[35,36] The Andersen–Pesavento–Wang model considers the problems in the Tanabe–Kaneko model and is more coherent with the experimental results and the numerical results from the direct numerical simulation of the Navier–Stokes equations.

However, Andersen et al. paid much attention to the phenomenology of their model but lacked close research in the simulation part. Without reliable numerical simulation near the heteroclinic bifurcation region, they only mentioned the possibility that the chaotic transition region found in experiments could be the heteroclinic bifurcation in their model. Moreover, it turned out in our simulation that the model cannot provide meaningful prediction in chaos by traditional numerical methods. Thus, we aim to conduct reliable numerical simulations to closely study the chaotic cases and heteroclinic bifurcation regions. The motivation of this paper is to implement a radical numerical strategy to empower the Andersen–Pesavento–Wang model with the ability to accurately predict trajectories in extremely sensitive cases.

In the present paper, the impact of numerical noises is eliminated by a novel approach. Liao[37] suggested a numerical strategy in 2009, namely, the "Clean Numerical Simulation" (CNS),[38,39] to overcome the limitations mentioned above of traditional algorithms in double precision. Employing the CNS, reliable/convergent numerical simulations of chaotic dynamical systems can be obtained in a controllable interval of time $0 \leq t \leq T_c$, where T_c is called the "critical predictable time." Compared with the traditional validated numerical methods like interval arithmetics,[40] the CNS is a practical numerical strategy. The implementation of MP makes it easier to use and computationally cheaper than interval arithmetic, while the convergence checks to determine T_c still practically ensure the reliability of computational results. This method has been proved to be effective to calculate reliable trajectories in many chaotic systems, including the Lorenz equation,[37] three-body system,[42–44] and also spatiotemporal chaos.[45,46] For example, by implementing the CNS, Li et al. successfully found more than 2000 new periodic orbits of the three-body problem, which was pointed out by Poincaré[5] as a classic chaotic system. Most of these periodic solutions are inaccessible by traditional means,[42–44] which illustrates the usefulness of the CNS as a powerful tool for reliable investigation of chaotic systems in physics with high fidelity. As for the spatiotemporal chaos, Lin et al.[45] used the CNS to control numerical noises smaller than the micro-level thermal fluctuations, by which it was proved that the inherent micro-level thermal fluctuations are the root source of macroscopic randomness of Rayleigh–Bénard turbulent convection flows. Hu et al.[46] developed a more efficient algorithm of the CNS to simulate the one-dimensional complex Ginzburg–Landau equation (CGLE). It further exhibits that the CNS method can accurately maintain both the statistical features of spatiotemporal systems and the symmetric characteristics of the solutions in which traditional numerical treatment has failed.

We organize this manuscript as follows. The Andersen–Pesavento–Wang model and the CNS strategy are briefly introduced in Sec. II. In Sec. III, we demonstrate the sensitivity of the free-fall

problem to numerical noises and the advantage of the CNS method by comprehensive comparisons from both chaotic and periodic simulations. Finally, we close with discussions and concluding remarks in the last section.

II. MATHEMATICAL MODEL AND NUMERICAL ALGORITHM

A. Andersen–Pesavento–Wang model

As shown in Fig. 1, the Andersen–Pesavento–Wang model is a comprehensive analytical model to predict the trajectories of a freely falling two-dimensional disk driven by gravity,

$$\begin{cases} I^* \dot{V}_{x'} = (I^* + 1)\dot{\theta} V_{y'} - \Gamma V_{y'} - \sin\theta - F_{x'}, \\ (I^* + 1)\dot{V}_{y'} = -I^* \dot{\theta} V_{x'} + \Gamma V_{x'} - \cos\theta - F_{y'}, \\ \frac{1}{4}\left(I^* + \frac{1}{2}\right)\ddot{\theta} = -V_{x'} V_{y'} - \tau, \end{cases} \tag{1}$$

with the coordinate transformation

$$\begin{cases} \dot{x} = V_{x'}\cos\theta - V_{y'}\sin\theta, \\ \dot{y} = V_{x'}\sin\theta + V_{y'}\cos\theta, \end{cases} \tag{2}$$

where the dot denotes the derivative with respect to the time t, (x', y') is the local coordinate fixed with the disk, (x, y) is the global (inertia) coordinate, $(V_{x'}, V_{y'})$ is the velocity of the disk in the local coordinate, and θ is the rotation angle of the disk; the circulation Γ is given by

$$\Gamma = \frac{2}{\pi}\left(-\frac{C_T V_{x'} V_{y'}}{\sqrt{V_{x'}^2 + V_{y'}^2}} + C_R \dot{\theta}\right), \tag{3}$$

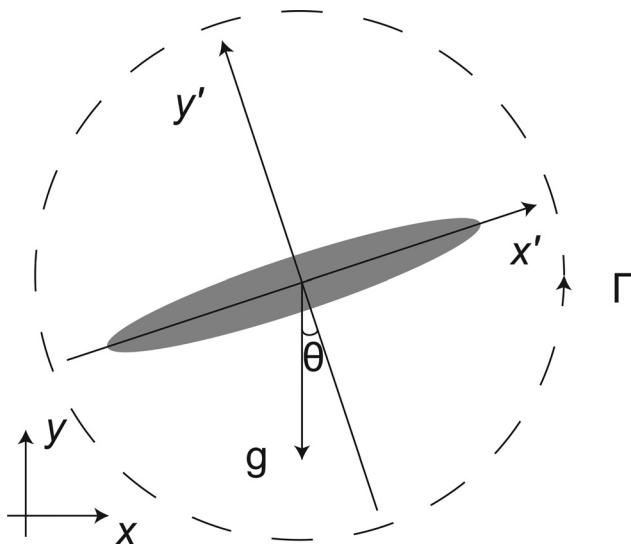and the viscous forces $(F_{x'}, F_{y'})$ and torque τ are given by

FIG. 1. The local reference frame (x', y') fixed with the disk and the global reference frame (x, y) of a freely falling two-dimensional desk, where θ denotes the rotation angle of the disk, g is the acceleration due to gravity, and Γ is the circulation.

$$(F_{x'}, F_{y'}) = \frac{1}{\pi}\left(A - B\frac{V_{x'}^2 - V_{y'}^2}{V_{x'}^2 + V_{y'}^2}\right)\sqrt{V_{x'}^2 + V_{y'}^2}(V_{x'}, V_{y'}),$$
$$\tau = (\mu_1 + \mu_2|\dot{\theta}|)\dot{\theta}, \tag{4}$$

respectively. All variables are dimensionless. This model has seven dimensionless parameters $I^*, C_T, C_R, A, B, \mu_1, \mu_2$, where $I^* = (\rho_s b)/(\rho_f a)$, with ρ_s, ρ_f being the densities of the disk and fluid and a, b the length of the semi-major and semi-minor axis of the elliptical disk, and other parameters are related to the geometry of the falling disk. For an elliptical disk,[35,36] we obtain

$$C_T = 1.2, \quad C_R = \pi, \quad A = 1.4, \quad B = 1.0, \quad \mu_1 = 0.2, \quad \mu_2 = 0.2 \tag{5}$$

by means of fitting the viscous forces and torques of experimental results and the direct numerical simulation of the Navier–Stokes equation. For details, refer to Refs. 35 and 36. In this paper, we use the Andersen–Pesavento–Wang model with the above-mentioned values of the parameters $C_T, C_R, A, B, \mu_1, \mu_2$. In this paper, we only adjust the parameter I^* to produce different falling modes of the disk.

B. Clean numerical simulation (CNS)

Generally, the CNS is able to obtain long-term reliable results thanks to its strategy to control the "numerical noises," say decrease the truncation errors to a required level by implementing numerical schemes with extremely high precision and control the round-off errors within a required range with all physical/numerical variables and parameters in multiple precision.

Truncation errors come from the discretization of continuous systems. The numerical methods have the following general form:

$$f(t + h) = f(t) + h \times RHS(t), \tag{6}$$

where $RHS(t)$ denotes the right-hand side. It varies according to the numerical methods. For the Nth order Runge–Kutta family method, N-step multi-step method, and Nth order Taylor series method, the right-hand side has the following general forms:

$$\begin{cases} RHS(t) = \sum_{i=1}^{N} k_i f(t_{k_i}) + O(h^N), \\ RHS(t) = \sum_{i=1}^{N} k_i f(t_{i-N-1}) + O(h^N), \\ RHS(t) = \sum_{i=1}^{N} \frac{f^{(i)}(t)}{i!} h^{i-1} + O(h^N). \end{cases} \tag{7}$$

$O(h^N)$ is the order of global truncation errors. The CNS is aimed to reduce the truncation errors so small that it would not damage the long-term prediction, either by reducing time steps h or increasing N with high-order methods. The round-off errors invariably arising with data are stored in computers in finite digits. We implemented the multiple-precision libraries (MP, called the MPFR library in the C language)[41] to also reduce the round-off errors to a small enough level.

By that, the numerical noises of the simulation are controlled arbitrarily small. To determine the critical predictable time T_c, one would conduct an additional simulation with even smaller numerical

noises. In a temporal dynamic system, we assume that numerical noises grow exponentially within an interval of time $t \in [0, T_c]$,

$$\mathcal{E}(t) = \mathcal{E}_0 \exp(\kappa t), \quad t \in [0, T_c], \tag{8}$$

where the constant $\kappa > 0$ is called the noise-growing exponent, which is coherent with the largest Lyapunov exponent (LLE), $\mathcal{E}_0$. It denotes the level of initial noises (i.e., truncation and round-off errors), and $\mathcal{E}(t)$ is the level of evolving noises of numerical simulation. Theoretically, a critical level of noise $\mathcal{E}_c$ determines the critical predictable time T_c by the equation

$$\mathcal{E}_c = \mathcal{E}_0 \exp(\kappa T_c). \tag{9}$$

It is obvious to tell from the above equation that the smaller initial noise $\mathcal{E}_0$ promises a longer T_c. Since the true orbits are impossible to get, the CNS implements a practical method to determine T_c. Let $\Phi(t)$ be a numerical simulation reliable in $t \in [0, T_c]$ with the initial noise $\mathcal{E}_0$ and $\Phi'(t)$ be another simulation (with the same physical parameters and the same initial conditions) in $t \in [0, T_c]$ with the initial noise $\mathcal{E}_0'$ that is several orders of magnitude smaller than $\mathcal{E}_0$. According to the hypothesis that numerical noises grow exponentially, it is sure that $T_c' > T_c$ and $\Phi'(t)$ in $t \in [0, T_c]$ should be much closer to the true orbit than $\Phi(t)$. Therefore, we use $\Phi'(t)$, a better simulation with less numerical noises, to decide T_c of $\Phi(t)$. After obtaining T_c of $\Phi(t)$, we can name safely that $\Phi(t)$ is clean numerical simulation (CNS) in $t \in [0, T_c]$. These, as mentioned earlier, provide us a heuristic explanation of the strategy of the CNS. The CNS also applies to non-hyperbolic chaotic systems.

We implement the above strategy to obtain the CNS results of the Andersen–Pesavento–Wang model. Given the discontinuous term in Eq. (4), we use a fixed step fourth order Runge–Kutta method with a strict time step in multiple precision. To determine T_c, an additional simulation is performed with even smaller time steps and more digits to store data in computer to guarantee that the extra simulation contains even less numerical noises. For the formal definition of T_c, we follow the form in Ref. 37. With the formula that $|1 - \frac{u_1}{u_2}| > \delta$, at $t = T_c$, where $\delta = 1\%$ in this paper, we determine the exact T_c of the Andersen–Pesavento–Wang model. In the following manuscript, we would like to demonstrate where and how numerical noises can harm the fidelity of trajectory prediction in the Andersen–Pesavento–Wang model.

III. ACCURATE PREDICTION GIVEN BY THE CNS

A. Chaotic trajectories

It was regarded that chaotic free-fall motion of disks in the water is long-term unpredictable by numerical simulation. In this section, we address that the CNS is able to provide long-term reliable prediction. We study the chaotic case with $I^* = 2.2$ reported by Andersen et al.[35,36] Four different types of initial conditions are considered for generality. These four initial conditions are listed in the form $(x, y, \theta, V_{x'}, V_{y'}, \dot{\theta})$ in Table I with their corresponding schematic diagram shown in Fig. 2.

Traditional methods are powerless as a prediction tool with chaos. In case 1, we computed trajectories by the fourth order Runge–Kutta method in double precision with different time steps from 1×10^{-2} to 1×10^{-7}. The trajectories are plotted in Fig. 3. It is found that all trajectories are divergent from each other after about $250 UT$. Although traditional numerical methods can obtain

TABLE I. The initial conditions of the four cases of chaotic falling.

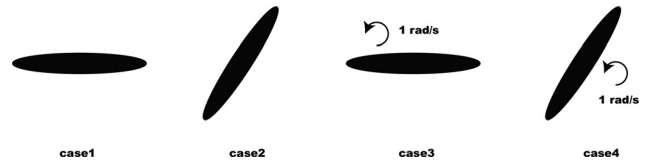| No.	Angle of attack	Rotation	$(x, y, \theta, V_{x'}, V_{y'}, \dot{\theta})$
1			$(0, 0, 0, 0, 0.01, 0)$
2	$\checkmark$		$(0, 0, 1, 0, 0.01, 0)$
3		$\checkmark$	$(0, 0, 0, 0, 0.01, 1)$
4	$\checkmark$	$\checkmark$	$(0, 0, 1, 0, 0.01, 1)$

FIG. 2. The schematic diagram of the four types of initial conditions considered. The four cases correspond to disks that fall from a static state with no angle of attack, that fall from a static state with an angle of attack, that fall from a rotational state with no angle of attack, and that fall from a rotational state with an angle of attack.

qualitatively correct chaotic trajectories, these trajectories are of little use from the aspect of prediction: it is impossible to tell which one should be used as the predicted trajectory. The CNS, on the other hand, is able to give true trajectories: the trajectory with $h = 1 \times 10^{-6}$ in 60-digits and that with $h = 1 \times 10^{-7}$ in 120-digits. Therefore, for a chaotic system, the reliable solution is too sensitive to be found by the traditional approach. The good thing is that CNS can perfectly circumvent this issue.

Without loss of generality, we consider the relationships between T_c and numerical noises in case 1. We have demonstrated that with $h = 1 \times 10^{-6}$ in 60-digits, the trajectory is clean. According to that, two sets of numerical experiments are conducted to consider the effect of truncation and round-off errors, respectively. The first set is designed to contain only truncation errors: thus, all data are stored in 60-digits, while the time steps are larger than $h = 1 \times 10^{-6}$. The second set is designed to contain only round-off errors: thus, the same time step $h = 1 \times 10^{-6}$ is implemented, but data are stored in less digits, from 16-digits (double precision) to around 25-digits. With the definition of T_c, we could compute T_c of these cases by comparing the trajectories with the clean trajectory computed with $h = 1 \times 10^{-6}$ in 60-digits. With these two sets of numerical experiments, we confirm that T_c of the Andersen–Pesavento–Wang model also applies to the exponential growth law. There exist linear relationships between T_c and the logarithm of time steps h, T_c, and the digits of data K. The quantitative results are given by the following equations:

$$T_c \approx \min\{10.95K + 96.11, -42.81 \log_{10} h + 112.56\}, \tag{10}$$

which provide a rough estimation of T_c of case 1. The exact T_c is decided by the minimum of T_c with truncation and round-off errors. Generally, with smaller time steps h and larger digits K, longer reliable prediction could be obtained. Also, it is able to estimate the time steps and digits needed for a certain T_c for the purpose of prediction (Fig. 4).

In all four cases, the CNS is able to provide convergent prediction of the exact falling trajectories of disks. Let us compare the differences
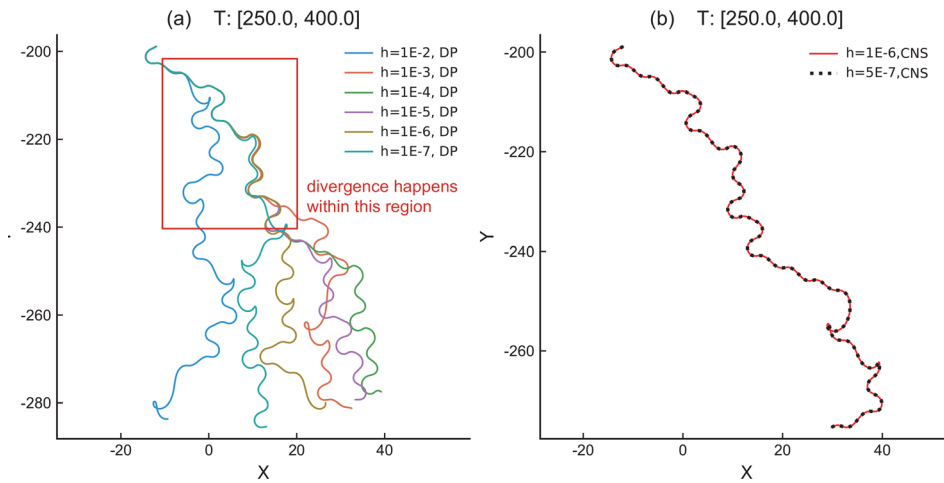
FIG. 3. (a) The trajectories of the same initial condition computed by the fourth order Runge–Kutta method in double precision with different time steps. All trajectories are divergent from each other, making these trajectories of little value a prediction. (b) The trajectories of the same initial condition but computed by the CNS. The black dotted trajectory is computed with smaller time steps and data stored in more digits, which proves that the red trajectory is "clean."
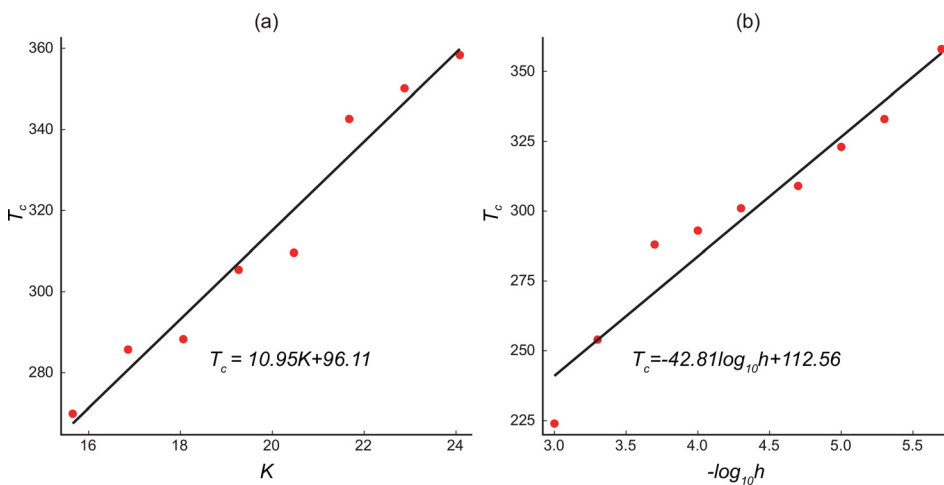

FIG. 4. (a) The linear relationships between T_c and decimal digits K; (b) the linear relationships between T_c and the logarithm of steps.

between the falling trajectories computed by the traditional methods and the CNS. The details of how trajectories computed by traditional methods diverge from the true trajectories of all four cases are demonstrated in Fig. 5. The trajectories in red are computed by traditional methods with $h = 1 \times 10^{-6}$, while the trajectories in black are computed by the CNS with the same time steps. In all our cases, the numerical noises first result in an observable phase difference of posture angle θ. Then, the phase difference continuously increases and finally develops into a different falling path, marking the failure of prediction. Among the four cases, the divergence happens at different times. The first case that disks fall from a static state with no angle of attack has the latest divergence because it takes the longest time for the initial condition to develop into chaos. Except for that, these four cases have the same qualitative phenomenon.

B. Heteroclinic bifurcation

In this section, we study the heteroclinic bifurcation region reported by Andersen et al. in their paper on the analysis of transition between fluttering and tumbling states.[36] They described it as a sharp transition, while the bifurcation regions are sensitive to noises. In their

work, Andersen et al. succeeded in studying the heteroclinic bifurcation to the precision of 1×10^{-5}. With the help of CNS, we approach the heteroclinic bifurcation region in even higher precision of 1×10^{-11} and provide reliable prediction, which was never reported before. It is worth noting that only the CNS can predict the falling modes in that high precision as shown in the following example.

Given the dynamical characteristics of the Andersen–Pesavento–Wang model, it has four steady solutions, corresponding to two fixed points where disk falls vertically, and gravity is balanced by drag,

$$
\begin{bmatrix} v_{x'} \\ v_{y'} \\ \theta \\ \dot{\theta} \end{bmatrix} = \begin{bmatrix} \mp\sqrt{\dfrac{\pi}{A-B}} \\ 0 \\ \dfrac{\pi}{2}, \dfrac{3\pi}{2} \\ 0 \end{bmatrix} = \begin{bmatrix} \mp V \\ 0 \\ \dfrac{\pi}{2}, \dfrac{3\pi}{2} \\ 0 \end{bmatrix}, \tag{11}
$$

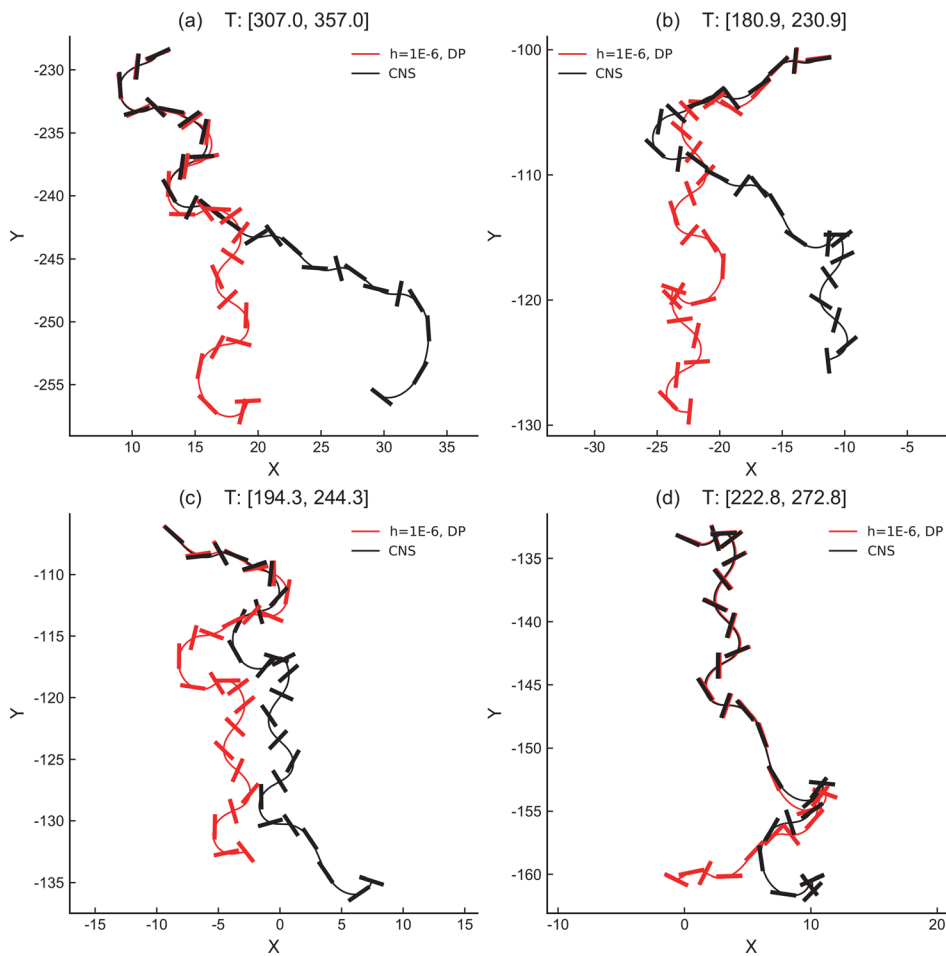and two other fixed points where the face of the disk is normal to the direction of motion,

FIG. 5. Comparison between trajectories computed by traditional methods vs that computed by the CNS. (a)–(d) correspond to case 1 to 4, respectively.

$$\begin{bmatrix} v_{x'} \\ v_{y'} \\ \theta \\ \dot{\theta} \end{bmatrix} = \begin{bmatrix} 0 \\ \mp\sqrt{\dfrac{\pi}{A+B}} \\ 0, \pi \\ 0 \end{bmatrix} = \begin{bmatrix} 0 \\ \mp W \\ 0, \pi \\ 0 \end{bmatrix}. \quad (12)$$

Andersen *et al.* discovered that the fluttering modes transform to tumbling modes via a heteroclinic bifurcation at a specific I_c^*, that is with I close to I_c^*, all disks with $I^* < I_c^*$ fall in fluttering modes, while disks with $I^* > I_c^*$ fall in tumbling modes, as shown in Fig. 6. So, mathematically, I_c^* is the critical parameter that decides disks' falling modes. Note that the periodicity of disks grows exponentially longer as I^* approaches I_c^*. Andersen *et al.* explained that the phenomenon results from heteroclinic bifurcation like the famous Shilnikov phenomenon.

With the help of the CNS, it is able to obtain an I^* value that is extremely close to I_c^* by a dichotomization process based on the fact that I_c^* must lie between fluttering and tumbling modes. For example, $I^* = 1.219\,146\,631\,202\,101\,5$ is very close to I_c^* with a precision of 1×10^{-11}. Its true trajectory is in fluttering modes computed by the CNS, plotted in Fig. 7. The CNS results can predict the falling modes

even in extremely high precision near the heteroclinic bifurcation point.

However, the trajectories computed by the traditional methods with different time steps (1×10^{-2}, 1×10^{-3}, and 1×10^{-4}) act chaotic as a Computational Chaos (CC) phenomenon, shown in Fig. 7. From the aspect of prediction, this means that traditional methods cannot predict the falling modes of trajectories near the bifurcation point. The CC addresses a loose similarity between the heteroclinic bifurcation region and the chaotic transition region.[21] However, note that when I^* is close to I_c^*, the periods are elongated. It is easy to find that the "chaotic" trajectories in Fig. 7 have the characteristics of periodicity, compared with the chaos discussed in Sec. III A and in Fig. 3. The obvious differences confirm that the heteroclinic bifurcation region and the chaotic transition region are different.

Considering the special characteristics of the CC here, it is worth for us to distinguish it from the classic CC proposed by Lorenz[47] as a new type. They have two main differences. First, this type of CC has characteristics of periodicity as mentioned. The uncertainty only occurs near the heteroclinic bifurcation point, which decides that the disk would either flutter or tumble in the next period. Therefore, we refer such chaos as heteroclinic bifurcation chaos. Second, the CC proposed by Lorenz is only caused by too large time steps and can be
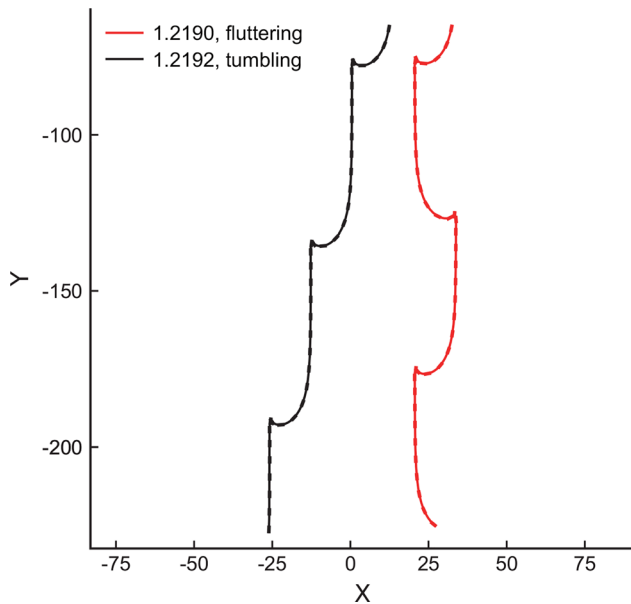
FIG. 6. Two characteristic trajectories near l_c^*. The trajectory with $l^* = 1.2190$ falls in fluttering modes, while the trajectory with $l^* = 1.2191$ falls in tumbling modes.

eliminated when traditional methods with smaller time steps are used. On the other hand, the CC found in the Andersen–Pesavento–Wang model is unavoidable when computed by traditional methods. No matter what time steps are picked, the CC always happens. This can
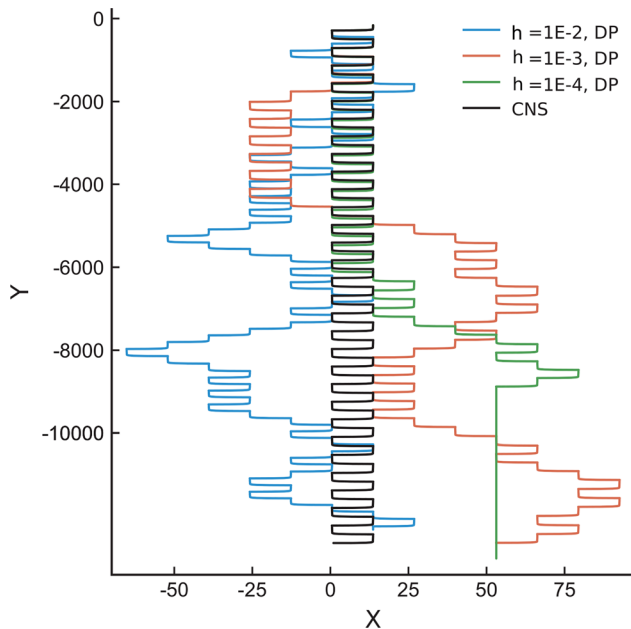

FIG. 7. The computational chaos resulted from numerical noises. The black line is the trajectory computed by the CNS, which falls in the fluttering modes. On the other hand, the trajectory computed by the fourth order Runge–Kutta method in double precision is neither fluttering nor tumbling. Instead, they are in a special type of chaos resulted.

be explained by the fact that such CC can be caused by both truncation errors and round-off errors, and so traditional methods are powerless to control these errors small enough to ensure that the simulation is clean.

Given the characteristics of heteroclinic bifurcation chaos, experimental noises, as pointed out by Andersen et al.,[36] could also trigger that heteroclinic bifurcation chaos in that region. We can only conclude that the heteroclinic bifurcation of the Andersen–Pesavento–Wang model is actually different from the chaotic transition region. However, we cannot preclude the existence of heteroclinic bifurcation chaos discovered here although it is strange that it was never reported before in any experiments of disks falling in the water. Whether this type of falling mode exists or the Andersen–Pesavento–Wang model is not correct as describing the transition between fluttering and tumbling is still an open question worth further study.

IV. DISCUSSIONS AND CONCLUDING REMARKS

In this paper, we show that the uncertainty of the numerical simulation of free-fall motion in the water can be overcome by a novel but powerful tool, the CNS. In the chaotic cases, numerical noises grow exponentially. Hence, even though they are as small as 1×10^{-16}, they are amplified exponentially. It is impossible to obtain long-term reliable prediction of chaotic free-fall motion in the water by means of traditional numerical algorithms in double precision unless the CNS is applied. Besides, in the heteroclinic bifurcation region, numerical noises can accumulate during the long period and destroy the bifurcation structure, acting like a new type of computational chaos. Under this circumstance, traditional methods cannot even predict the disk's falling modes. Although numerical noises can ruin the validity of this problem, a good way to control them at a small enough level can still give us a trustful and reliable result in a long enough interval of time.

In the past, the role of numerical noises was usually neglected. It is magnificent that we implement physical models to simulate and predict versatile phenomena in the nature, but it is not recommended to draw conclusions without the awareness of the fidelity of the simulation. Take the re-entry problem as an example. In this kind of big engineering project, no doubt a better prediction of the landing spot will bring tremendous economic and safety benefits. Hence, this work shows people a correct direction to radically solve chaotic problems by numerical methods, and it is of practical importance.

ACKNOWLEDGMENTS

DATA AVAILABILITY

The data that support the findings of this study are available from the corresponding author upon reasonable request.

REFERENCES

[1]J. Tang, L. Liu, H. Cheng, S. Hu, and J. Duan, "Long-term orbit prediction for Tiangong-1 spacecraft using the mean atmosphere model," Adv. Space Res. **55** (5), 1432–1444 (2015).

[2]R. W. Powell, "Six-degree-of-freedom guidance and control-entry analysis of the HL-20," J. Spacecr. Rockets **30**(5), 537–542 (1993).

[3]C. Zimmerman, G. Dukeman, and J. Hanson, "Automated method to compute orbital reentry trajectories with heating constraints," J. Guid., Control, Dyn. **26** (4), 523–529 (2003).

[4]V. S. Aslanov and A. S. Ledkov, "Chaotic motion of a reentry capsule during descent into the atmosphere," J. Guid., Control, Dyn. **39**(8), 1834–1843 (2016).

[5]H. Poincaré, "Sur le problème des trois corps et les équations de la dynamique," Acta Math. **13**(1), A3–A270 (1890).

[6]E. N. Lorenz, "Deterministic nonperiodic flow," J. Atmos. Sci. **20**(2), 130–141 (1963).

[7]J. C. Sprott, *Elegant Chaos: Algebraically Simple Chaotic Flows* (World Scientific, 2010).

[8]J. C. Sprott and J. C. Sprott, *Chaos and Time-Series Analysis* (Citeseer, 2003), Vol. 69.

[9]E. N. Lorenz, "Computational periodicity as observed in a simple system," Tellus A **58**(5), 549–557 (2006).

[10]J. Teixeira, C. A. Reynolds, and K. Judd, "Time step sensitivity of nonlinear atmospheric models: Numerical convergence, truncation error growth, and ensemble design," J. Atmos. Sci. **64**(1), 175–189 (2007).

[11]J. C. Maxwell, "On a particular case of the descent of a heavy body in a resisting medium," Cambridge Dublin Math. J **9**, 145–148 (1854).

[12]F. Auguste, J. Magnaudet, and D. Fabre, "Falling styles of disks," J. Fluid Mech. **719**, 388–405 (2013).

[13]M. Chrust, G. Bouchet, and J. Dušek, "Numerical simulation of the dynamics of freely falling discs," Phys. Fluids **25**(4), 044102 (2013).

[14]C. Toupoint, P. Ern, and V. Roig, "Kinematics and wake of freely falling cylinders at moderate Reynolds numbers," J. Fluid Mech. **866**, 82–111 (2019).

[15]K. Amin, J. Mac Huang, K. J. Hu, J. Zhang, and L. Ristroph, "The role of shape-dependent flight stability in the origin of oriented meteorites," Proc. Natl. Acad. Sci. **116**(33), 16180–16185 (2019).

[16]J.-T. Kim, Y. Jin, S. Shen, A. Dash, and L. P. Chamorro, "Free fall of homogeneous and heterogeneous cones," Phys. Rev. Fluids **5**(9), 093801 (2020).

[17]L. B. Esteban, J. Shrimpton, and B. Ganapathisubramani, "Edge effects on the fluttering characteristics of freely falling planar particles," Phys. Rev. Fluids **3** (6), 064302 (2018).

[18]L. B. Esteban, J. Shrimpton, and B. Ganapathisubramani, "Three dimensional wakes of freely falling planar polygons," Exp. Fluids **60**(7), 114 (2019).

[19]S. P. Kuznetsov, "Plate falling in a fluid: Regular and chaotic dynamics of finite-dimensional models," Regular Chaotic Dyn. **20**(3), 345–382 (2015).

[20]W. W. Willmarth, N. E. Hawk, and R. L. Harvey, "Steady and unsteady motions and wakes of freely falling disks," Phys. Fluids **7**(2), 197–208 (1964).

[21]S. B. Field, M. Klaus, M. Moore, and F. Nori, "Chaotic dynamics of falling disks," Nature **388**(6639), 252–254 (1997).

[22]H. Zhong, C. Lee, Z. Su, S. Chen, M. Zhou, and J. Wu, "Experimental investigation of freely falling thin disks. Part 1. The flow structures and Reynolds number effects on the zigzag motion," J. Fluid Mech. **716**, 228 (2013).

[23]H. Zhong, S. Chen, and C. Lee, "Experimental study of freely falling thin disks: Transition from planar zigzag to spiral," Phys. Fluids **23**(1), 011702 (2011).

[24]C. Lee, Z. Su, H. Zhong, S. Chen, M. Zhou, and J. Wu, "Experimental investigation of freely falling thin disks. Part 2. Transition of three-dimensional motion from zigzag to spiral," J. Fluid Mech. **732**, 77–104 (2013).

[25]Y. Wang, C. Shu, C. Teo, and L. Yang, "An efficient immersed boundary-lattice Boltzmann flux solver for simulation of 3D incompressible flows with complex geometry," Comput. Fluids **124**, 54–66 (2016).

[26]Y. Wang, C. Shu, C. Teo, and L. Yang, "Numerical study on the freely falling plate: Effects of density ratio and thickness-to-length ratio," Phys. Fluids **28** (10), 103603 (2016).

[27]T. Kim, J. Chang, and D. Kim, "Free-fall dynamics of a pair of rigidly linked disks," Phys. Fluids **30**(3), 034104 (2018).

[28]M. Lee, S. H. Lee, and D. Kim, "Stabilized motion of a freely falling bristled disk," Phys. Fluids **32**(11), 113604 (2020).

[29]G. Kirchhoff, "Ueber die bewegung eines rotationskörpers in einer flüssigkeit," J. Reine Angew. Math. **71**, 237–262 (1870).

[30]A. V. Borisov and I. S. Mamaev, "On the motion of a heavy rigid body in an ideal fluid with circulation," Chaos **16**(1), 013118 (2006).

[31]A. V. Borisov, V. V. Kozlov, and I. S. Mamaev, "Asymptotic stability and associated problems of dynamics of falling rigid body," Regular Chaotic Dyn. **12**(5), 531–565 (2007).

[32]Y. Tanabe and K. Kaneko, "Behavior of a falling paper," Phys. Rev. Lett. **73** (10), 1372 (1994).

[33]L. Mahadevan, H. Aref, and S. Jones, "Comment on "Behavior of a falling paper,"" Phys. Rev. Lett. **75**(7), 1420 (1995).

[34]Y. Tanabe and K. Kaneko, "Behavior of a falling paper," Phys. Rev. Lett. **75**(7), 1421 (1995).

[35]A. Andersen, U. Pesavento, and Z. J. Wang, "Analysis of transitions between fluttering, tumbling and steady descent of falling cards," J. Fluid Mech. **541**(1), 91–104 (2005).

[36]A. Andersen, U. Pesavento, and Z. J. Wang, "Unsteady aerodynamics of fluttering and tumbling plates," J. Fluid Mech. **541**(1), 65 (2005).

[37]S. Liao, "On the reliability of computed chaotic solutions of non-linear differential equations," Tellus A **61**(4), 550–564 (2008).

[38]S. Liao, "On the numerical simulation of propagation of micro-level inherent uncertainty for chaotic dynamic systems," Chaos, Solitons Fractals **47**, 1–12 (2013).

[39]S. Liao, "Physical limit of prediction for chaotic motion of three-body problem," Commun. Nonlinear Sci. Numer. Simul. **19**(3), 601–616 (2014).

[40]W. Tucker, *Validated Numerics: A Short Introduction to Rigorous Computations* (Princeton University Press, 2011).

[41]P. Oyanarte, "MP: A multiple precision package," Comput. Phys. Commun. **59**, 345–358 (1990).

[42]X. Li and S. Liao, "More than six hundred new families of Newtonian periodic planar collisionless three-body orbits," Sci. China Phys., Mech. Astron. **60**(12), 129511 (2017).

[43]X. Li, Y. Jing, and S. Liao, "Over a thousand new periodic orbits of a planar three-body system with unequal masses," Publ. Astron. Soc. Jpn. **70**(4), 64 (2018).

[44]X. Li and S. Liao, "Collisionless periodic orbits in the free-fall three-body problem," New Astron. **70**, 22–26 (2019).

[45]Z. Lin, L. Wang, and S. Liao, "On the origin of intrinsic randomness of Rayleigh–Bénard turbulence," Sci. China Phys., Mech. Astron. **60**(1), 014712 (2017).

[46]T. Hu and S. Liao, "On the risks of using double precision in numerical simulations of spatio-temporal chaos," J. Comput. Phys. **418**, 109629 (2020).

[47]E. N. Lorenz, "Computational chaos-a prelude to computational instability," Physica D **35**(3), 299–317 (1989).